$\mathcal{PT}$ Symmetry with a System of Three-Level Atoms

Chao Hang,[1] Guoxiang Huang,[1] and Vladimir V. Konotop[2]

[1]State Key Laboratory of Precision Spectroscopy and Department of Physics, East China Normal University, Shanghai 200062, China
[2]Centro de Física Teórica e Computacional and Departamento de Física, Faculdade de Ciências, Universidade de Lisboa, Avenida Professor Gama Pinto 2, Lisboa 1649-003, Portugal

(Received 22 September 2012; published 21 February 2013)

We show that a vapor of multilevel atoms driven by far-off-resonant laser beams, with the possibility of interference of two Raman resonances, is highly efficient for creating parity-time symmetric profiles of the probe-field refractive index, whose real part is symmetric and imaginary part is antisymmetric in space. The spatial modulation of the probe-field susceptibility is achieved by a proper combination of standing-wave strong control fields and of Stark shifts induced by far-off-resonance laser fields. As particular examples we explore a mixture of isotopes of rubidium atoms and design a parity-time symmetric lattice and a parabolic refractive index with a linear imaginary part.

DOI: 10.1103/PhysRevLett.110.083604 PACS numbers: 42.50.Gy, 11.30.Er, 42.65.An

While non-Hermitian operators obeying pure real spectra, for example the Bogoliubov–de Gennes [1] equations, linear stability problem for nonlinear waves, or simply a parabolic potential with linear imaginary part [2], have been known in physics for a long time, it was only due to Ref. [3] that the fundamental importance of such operators became widely recognized. It was discovered in Ref. [3] that there exists a wide class of complex potentials of the Schrödinger equation obeying pure real spectra, and that this property is intrinsically related to the parity ($\mathcal{P}$) and time ($\mathcal{T}$) symmetries of physical systems. This discovery triggered the discussion [4] on the fundamentals of quantum mechanics whose axioms are based on Hermitian operators for observables. Further growth of interest in the theory of parity-time ($\mathcal{PT}$) symmetric potentials was originated by suggestions of implementation of $\mathcal{PT}$ symmetry in a waveguide with gain and absorption [5], on the basis of the analogy between quantum mechanics and optics where the refractive index plays the role of the potential in the Schrödinger equation. In optics a $\mathcal{PT}$-symmetric refractive index obeying gain and loss has been experimentally realized using four-wave mixing in an Fe-doped $LiNbO_3$ substrate [6]. The possibility of optical realization of $\mathcal{PT}$-symmetric potentials motivated various suggestions of practical applications, such as nonreciprocal wave propagation [6–8], implementation of a coherent perfect absorber [9], and giant wave amplification [10]. Experimental realization of $\mathcal{PT}$ symmetry using plasmonics [11] and synthetic lattices using optical couplers [12] were also reported.

The mentioned experimental observations of the $\mathcal{PT}$ symmetry were either performed in pure dissipative waveguides (see Refs. [8,13]) whose $\mathcal{PT}$ interpretation relies on the linearity of the system, which allows for scaling out the average decay of the field, or in systems having gain and loss localized in the transverse direction leading to an effectively discrete system whose description is reduced to a $\mathcal{PT}$-symmetric dimer, i.e., to coupled hot and cold spots (see Refs. [6,11]). The goal of this Letter is to show that using an alternative optically active media, namely vapors of multilevel atoms driven by control fields with proper Raman resonances and by a far-off-resonant laser field, it is possible to create a *spatially distributed* $\mathcal{PT}$-symmetric refractive index, i.e., one having the property $n(x) = n^*(-x)$, with n being the probe-field refractive index.

To this end we start by recalling recent achievements in the creation of large susceptibilities in atomic vapors controlled by external laser beams. While such systems are intrinsically dissipative, it was suggested in Ref. [14] and shown experimentally in Ref. [15] that, using the destructive interference in the imaginary part of susceptibility, it is possible to achieve large real refractive indexes while keeping the absorption small enough. Recently, the idea of using two far-off-resonant control fields for realizing high susceptibility with nearly zero absorption of a probe field was developed theoretically [16] and confirmed experimentally [17]. An alternative way of achieving a similar effect was proposed in Ref. [18] where two Λ systems were explored for exciting two Raman resonances (see also Ref. [19]).

Because the above mentioned schemes use the interference of two Raman resonances, one of which results in gain and another in absorption, the imaginary part of the probe-field susceptibility appears as a nonmonotonic function of the frequency with both positive (gain) and negative (absorbing) domains. An even more remarkable property is the possibility to design distributions where real and imaginary parts of the susceptibility appear, respectively, as even and odd functions of the probe-field frequency [16–19]. Because for a monochromatic beam the change $\omega \to -\omega$ is equivalent to the change $t \to -t$, the last property can be viewed as a *time inversion symmetry*. Thus our goal can be formulated as completing this symmetry by the *symmetry in the coordinate space*.

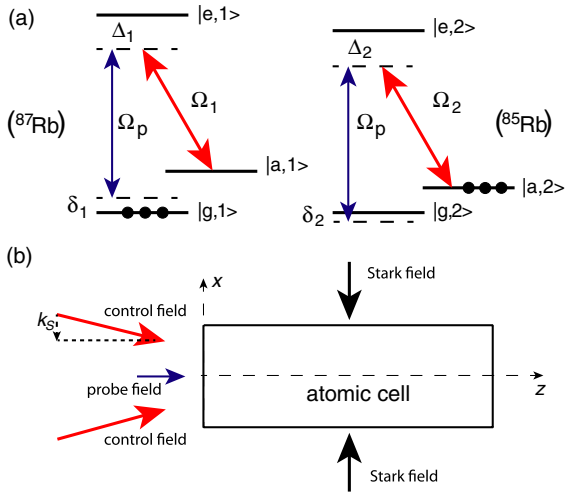

FIG. 1 (color online). (a) Two Λ systems and Raman transitions used for obtaining a $\mathcal{PT}$-symmetric refractive index. Initially populated levels are indicated by the filled circles. (b) Possible geometry for the suggested scheme. All notations are defined in the text.

To achieve this goal we choose a scheme based on a mixture of two species of Λ atoms, similar to the one explored in Ref. [18]. The involved atomic states will be assigned as $|g, s\rangle$ (ground state), $|a, s\rangle$ (lower state), and $|e, s\rangle$ (excited state), and hereafter $s = 1, 2$ indicates the species of the atoms (see Fig. 1). The species have atomic densities N_1 and N_2, respectively ($N = N_1 + N_2$ being total atomic density). Ω_p is the half Rabi frequency of the probe-field coupling $|g, s\rangle \leftrightarrow |e, s\rangle$, and $\Omega_{1,2}$ are half Rabi frequencies of two control fields coupling $|a, s\rangle \leftrightarrow |e, s\rangle$. All fields are far-off resonant, which is guaranteed by the condition $\Delta_s \gg \Omega_s$, where $\Delta_s = \omega_{e,s} - \omega_{a,s} - \omega_c$ is the one-photon detuning, with $\hbar\omega_{l,s}$ ($l = g, a, e$) being the eigenenergy of the state $|l, s\rangle$ and ω_p (ω_c) being the center frequency of the probe (control) field. Notice that one can explore different cases by changing the signs of the two-photon detuning, defined by $\delta_s = \omega_{a,s} - \omega_{g,s} - (\omega_p - \omega_c)$. In Fig. 1(a) we show the proposed scheme where $\delta_1 > 0$ and $\delta_2 < 0$, which corresponds to the $\mathcal{PT}$-symmetric lattice obtained below. In our configuration, the first scheme ($s = 1$) exhibits two-photon absorption for the probe field while the second one ($s = 2$) provides two-photon gain.

Spatial modulation of the probe-field susceptibility can be achieved by using x-dependent control fields [with half Rabi frequency $\Omega_s(x)$]. Such fields, however, affect both one- and two-photon detunings. Therefore we explore the second possibility, which is the modulation of relative energy-level shifts along the x direction, resulting in the dependence $\Delta_s = \Delta_s(x)$. This task can be achieved if a strong, far-detuned, continuous-wave laser field $E_S(x) \times \cos(\omega_S t)$, where E_S and ω_S are, respectively, amplitude and frequency, is applied to the system. This field originates the Stark shifts of energy levels with the expression $\Delta E_{S,s}(x) = -\frac{1}{4}\alpha_{l,s}E_S^2(x)$, where $\alpha_{l,s}$ is the scalar polarizability of the level $|l, s\rangle$. Below $E_S(x)$ is referred to as the Stark field. If within the required accuracy one can consider $\alpha_{g,s} \approx \alpha_{a,s}$, i.e., that the difference of Stark shifts between the ground-state sublevels is negligible (this is the situation we consider below), then δ_s is not affected by the Stark field while $\Delta_s(x) = \Delta_s - (\alpha_{e,s} - \alpha_{g,s})E_S^2(x)/(4\hbar)$. Thus the Stark field allows one to manipulate the spatial distribution of the one-photon detunings $\Delta_s(x)$, on the one hand, and, on the other hand, being far-off resonant does not lead to the power broadening of lines due to the low rate of transitions [20].

Because the Stark shift usually appears in the second order of the perturbation theory, it requires relatively strong electric fields. Taking into account the characteristics of available lasers, this may impose strong limitations, because the characteristic scale of the spatial modulation of $\Delta_s(x)$ is of the order of the wavelength of the Stark field λ_S. For the typical order of the control-field amplitudes $E_c \sim 10^2$ V/cm ($\Omega_{1,2} \sim 2\pi \times 514$ MHz), the required amplitude of the Stark field must be 3 orders of magnitude larger, i.e., $E_S \sim 10^5$ V/cm (for more detailed estimates see below). Being focused into a spot with diameter ≈ 30 μm, this requires laser powers on the order of 100 W. Nowadays such powers can be achieved using, say, quantum cascade lasers [21,22] operating at micron wavelengths (in Ref. [21] it was $\lambda_S = 4.45$ μm, which will be used in our estimates).

For the described model the susceptibility of the probe field is computed from the density-matrix formalism within the rotating-wave approximation and has a similar functional form as obtained in Ref. [18]. However, an essential difference appears here: to introduce spatial symmetry we use x-dependent control fields $\Omega_{1,2}(x)$ and an additional Stark field resulting spatial dependence of the one-photon detunings $\Delta_{1,2}(x)$. Thus we have

$$\frac{\chi_p(x)}{\chi_0} = \frac{\delta_1 - i\gamma_{ag}}{[\delta_1 + \Delta_1(x) - i\gamma_{eg}](\delta_1 - i\gamma_{ag}) - |\Omega_1(x)|^2} - \eta\frac{|\Omega_2(x)|^2[\Delta_2(x) + i\gamma_{ea}]^{-1}}{[\delta_2 + \Delta_2(x) - i\gamma_{eg}](\delta_2 - i\gamma_{ag}) - |\Omega_2(x)|^2}. \quad (1)$$

Here $\chi_0 = N_1 d_{eg,1}^2/(\varepsilon_0\hbar)$ and $\eta = N_2 d_{eg,2}^2/N_1 d_{eg,1}^2$ characterizethe ratio between the species densities considered as a free parameter, with ε_0 being the vacuum permittivity and $d_{eg,s}$ standing for the dipole moment of the transition between the ground and excited states of the sth system.

Generally speaking, in a warm vapor large Doppler broadened line widths (typically $\Delta\omega/\omega \sim 10^{-6}$ [20]) may degrade the effectiveness of resonant schemes. In our case, such broadening would not be important for large one-photon detunings as it is of the order of the

two-photon detunings. It turns out, however, that the effect of this line broadening can be significantly suppressed (by the factor $|\omega_c - \omega_p|/\omega_c$) if far-off-resonant copropagating beams (see, e.g., Ref. [23]) with frequencies close enough are used. This is the case we will consider below.

Now our task is to determine the spatial distributions of $\Omega_s(x)$ and $\Delta_s(x)$ ensuring the condition

$$\nu(x) \equiv n(x) - n^*(-x) = 0, \tag{2}$$

where $n(x) = n_r(x) + in_i(x) \approx 1 + \frac{1}{2}\chi_p(x)$, with x being either arbitrary or belonging to some intervals (see below). Unlike in the previous studies [16–18], where n was spatially independent and the parameters ensuring the enhanced reality of the refractive index were in focus, here we are interested in a somehow opposite situation and look for the parameters where the imaginary part of the refractive index is appreciable and at the same time satisfies the symmetry relation equation (2).

Because of the complexity of the relations among all parameters involved in Eqs. (1) and (2), it is not obvious *a priori* that the problem has a solution. Therefore we proceed with an analysis of particular systems. To this end we adopt the approach as follows. First, we define a seed susceptibility, with the shape we would like to obtain, say, $\chi^{sd}(x, \epsilon_j, \eta)$, which contains a number of free parameters ϵ_j and η. Second, neglecting all terms within some accuracy, say, of 10%, we compute analytical solutions for $\Omega_s^{sd}(x, \epsilon_j, \eta)$ and $\Delta_s^{sd}(x, \epsilon_j, \eta)$ from Eq. (2). Third, we substitute the obtained seed Rabi frequencies and Stark shifts in Eq. (1). Due to the crude approximations we made, the so-obtained susceptibility may still give significant errors in Eq. (2). Our final step is to minimize the error function $\nu(x, \epsilon_j, \eta)$ using the control parameters ϵ_j and η.

We first apply the above algorithm to obtain a $\mathcal{PT}$-symmetric lattice. Because the main limitation for the lattice period is determined by the Stark field, we require the period to be λ_S, i.e., $\chi(x) = \chi(x + \lambda_S)$. The experimental geometry we bear in mind is illustrated in Fig. 1(b). We further assume that each control field consists of two almost parallel plane waves having x components of the wave vector equal to $k_S = 2\pi/\lambda_S$, i.e., to the Stark-field wave vector. The seed solution can be chosen as $\chi^{sd} = \epsilon_0 + \epsilon_1 \cos\xi + i\epsilon_2 \sin\xi$, where $\xi = k_S x$ and $\epsilon_{0,1,2}$ are free parameters. As a particular atomic vapor, we use a mixture of isotopes ^{87}Rb($s = 1$) and ^{85}Rb($s = 2$) and assign $|g, s\rangle = |5S_{1/2}, F = 1\rangle$, $|a, s\rangle = |5S_{1/2}, F = 2\rangle$, and $|e, s\rangle = |5P_{1/2}, F = 1\rangle$ for each species.

To perform a numerical study, we further particularize the problem by assuming that $N_1 = 1.73 \times 10^{15}$ cm^{-3} and $N_2 = 1.57 \times 10^{15}$ cm^{-3} (thus $N = 3.30 \times 10^{15}$ cm^{-3}). The isotopes are loaded in a cell at approximately 363 K and the coherence decay rates are estimated as $\gamma_{eg} \approx \gamma_{ea} = 2\pi \times 334$ MHz and $\gamma_{ag} = 2\pi \times 16$ kHz [18]. With sufficiently high accuracy we can impose $\alpha_{e,1} - \alpha_{g,1} \approx \alpha_{e,2} - \alpha_{g,2} = 2\pi\hbar \times 0.1223$ Hz(cm/V)^2 and $d_{eg,1} \approx d_{eg,2} = 2.5377 \times 10^{-27}$ C cm [24], which allows us to consider $\Omega_1 \approx \Omega_2 = \Omega_c$. Other parameters are chosen as $\omega_p \approx \omega_c = 2\pi \times 3.77 \times 10^{14}$ s^{-1} ($\lambda_p = 795$ nm), $\eta = 0.91$, $\chi_0 = 0.57\gamma_{eg}$, $\delta_1 = 1.80\gamma_{eg}$, and $\delta_2 = -0.01\gamma_{eg}$. Then we solve equation $\chi_p(\Omega_s^{sd}, \Delta_s^{sd}) = \chi^{sd}$ with respect to the real Ω_s^{sd} and Δ_s^{sd}. For $|\delta_2| \ll |\delta_1|$ it is possible to leave only the leading terms in δ_2 allowing one to find the solutions explicitly. Finally, we substitute Ω_s^{sd} and Δ_s^{sd} back into Eq. (1) and make $\nu(x)$ as small as possible by tuning the parameters $\epsilon_{0,1,2}$. Because the obtained formulas have rather cumbersome forms they are not presented here. Instead, we write down the final expressions for the control-field Rabi frequency and for the Stark-field amplitude by keeping the first significant harmonics (i.e., the terms $\gtrsim 10^{-4}$),

$$E_S = E_0[0.9698 + 0.0053\cos\xi - 0.0007\sin\xi],$$
$$\Omega_c = \gamma_{eg}[1.5384 + 0.0122\cos\xi + 0.0232\sin\xi],$$

where $E_0 = 4 \times 10^5$ V/cm [see Fig. 2(a)]. As we already mentioned, the final shape of the susceptibility differs from the ansatz χ^{sd}. We represent it also in a form of a Fourier series by keeping the first significant harmonics, i.e., $\chi_p(x) = \chi_{0p} + \chi_{1p}(x)$, where $\chi_{0p} \approx 0.2257$ determines the average (in space) refractive index and the periodic part is given by

$$\chi_{1p} \approx 0.0075\cos\xi + 10^{-4}[1.2244\cos(2\xi) + i3.9418\sin\xi]. \tag{3}$$

The real and imaginary parts of the refractive index are shown in Fig. 2(b). We notice that there is a large difference between the magnitudes of the constant real part of the susceptibility and its imaginary part. What is important, however, is that the latter constitutes about 5% of the variation of the real part. The real and imaginary parts of the error function $\nu(x)$ are approximately 1% and 2% of the respective parts of $n(x)$.

Now we consider the propagation of the probe field along the z direction in the described atomic vapor. Because in the y direction the medium is homogeneous, in the paraxial approximation the beam propagation is governed by the

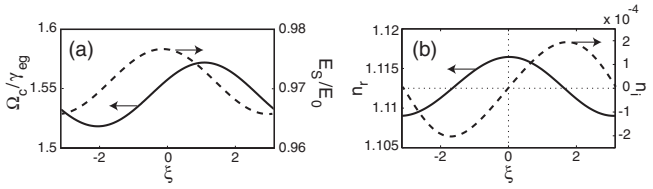

FIG. 2. (a) Spatial distributions of the control (solid line) and Stark (dashed line) fields required for producing the $\mathcal{PT}$-symmetric lattice. (b) Spatial distributions of the real (solid line) and imaginary (dashed line) parts of the refractive index.

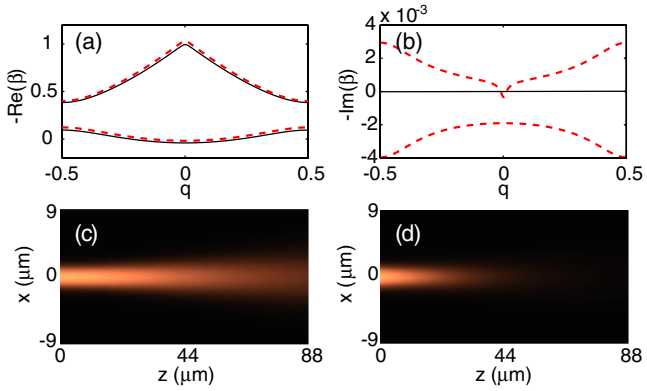

FIG. 3 (color online). Real (a) and imaginary (b) parts of the dimensionless propagation constant β. Solid and dashed lines show the results of a $\mathcal{PT}$-symmetric refractive index and a non-$\mathcal{PT}$-symmetric refractive index obtained by a change of the mutual concentration of species, as explained in the text. Evolution of $|\Omega_p(z)|^2$ in the vapors with $\mathcal{PT}$-symmetric (c) and non-$\mathcal{PT}$-symmetric (d) refractive indexes.

equation $2ik_p\frac{\partial\Omega_p}{\partial z}+\frac{\partial^2\Omega_p}{\partial x^2}+k_p^2\chi_{1p}(x)\Omega_p=0$, where $k_p=\frac{\omega_p}{c}\sqrt{1+\chi_{0p}}$ is the probe-field wave vector. The beam of constant amplitude in the y direction is chosen only for convenience; one can consider any waveguide structure in the y direction that results only in the renormalization of the constants in this equation. By the ansatz $\Omega_p(x,z)=\tilde{\Omega}(x)e^{ibz}$, where b is the propagation constant, we obtain $\frac{d^2\tilde{\Omega}}{d\xi^2}+\frac{k_p^2}{k_S^2}\chi_{1p}(\xi)\tilde{\Omega}=\beta\tilde{\Omega}$, where $\beta=\frac{2k_p}{k_S^2}b$. Taking into account the well-known results on periodic potentials [25] and rapid decay of Fourier harmonics in the expansion equation (3), one expects that with high accuracy the spectrum of β is indeed pure real. To check this, in Figs. 3(a) and 3(b) we show β obtained numerically for the susceptibility including all terms until the leading ones violate the condition in Eq. (2) (the latter have amplitudes $\lesssim 10^{-5}$).

Let us now show that the described procedure is structurally stable, i.e., that small deviations of system parameters do not break the obtained $\mathcal{PT}$ symmetry. To this end, we test the method with respect to the change of mutual concentration of the species. More specifically we have changed the obtained η by 10% and repeated the calculation described by the above algorithm (i.e., we did not use η as a matching parameter any more). We indeed find that now the accuracy with which the condition in Eq. (2) is satisfied is lower [see Figs. 3(a) and 3(b)] but the imaginary parts are still very small (of the order of 10^{-3} [26]). In Fig. 3 we also illustrate the propagation for an input Gaussian beam in the discussed $\mathcal{PT}$-symmetric [Fig. 3(c)] and non-$\mathcal{PT}$-symmetric [Fig. 3(d)] structures. The input probe beam $\Omega_p(z=0)=e^{-0.1(k_Sx)^2}$ propagates a much longer distance in the $\mathcal{PT}$-symmetric medium compared to that in the non-$\mathcal{PT}$-symmetric one where absorption is observed.

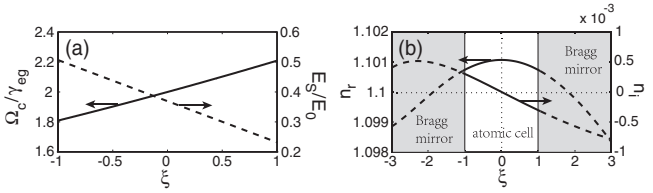

FIG. 4. (a) Spatial distributions of the control (solid line) and Stark (dashed line) fields required for producing the local $\mathcal{PT}$ symmetry. (b) Spatial distributions of the real and imaginary parts of the refractive index. Solid (dashed) lines show the refractive index inside (outside) the atomic cell limited by Bragg mirrors.

The described approach can be modified to produce other shapes of the refractive index. To illustrate this, now we show how to obtain a $\mathcal{PT}$-symmetric parabolic refractive index [2]. The main idea is based on the fact that $\mathcal{PT}$ symmetry can be satisfied only locally in space. Then one can cut undesirable non-$\mathcal{PT}$-symmetric distribution of the refractive index by choosing the location of the finite-size vapor cell with respect to the domain where the control and Stark fields produce local $\mathcal{PT}$ symmetry. We still consider the mixture of the rubidium isotopes, but now taking ^{85}Rb as the first ($s=1$) and ^{87}Rb as the second ($s=2$) systems. We choose $N_1=5.01\times 10^{18}$ cm^{-3} and $N_2=1.88\times 10^{16}$ cm^{-3}, $\eta=0.375\times 10^{-2}$, $\delta_1=3.56\times 10^{-4}\gamma_{eg}$, and $\delta_2=3.93\times 10^{-3}\gamma_{eg}$, without changing the other parameters. The described procedure of the choice of the control and Stark fields is performed to satisfy Eq. (2) only locally in space. In particular, this is achieved by taking $\Omega_c=\gamma_{eg}(2+0.2\xi+0.009\xi^2)$ and $E_S=E_0(0.3695-0.1375\xi)$, illustrated in Fig. 4(a). The spatial modulation of the refractive index now has a complex form, illustrated in Fig. 4(b). If the atomic cell (limited, say, by Bragg mirrors) is situated as shown in Fig. 4(b), the refractive index inside the cell, with the real and imaginary parts being, respectively, parabolic and linear, ensures the condition of Eq. (2) with very high accuracy. The real and imaginary parts of the error function $\nu(x)$ are approximately 0.2% and 0.4% of the respective parts of $n(x)$. The susceptibility inside the cell is described by $\chi_p=0.2021-0.0007\xi^2-i0.0006\xi$, which obviously satisfies the condition of $\mathcal{PT}$ symmetry.

To conclude, we suggested a possibility of creating $\mathcal{PT}$-symmetric profiles of the refractive index in a mixture of near resonant atomic gases. An important property of the proposed scheme is the possibility of generating various index profiles in one vapor and changing the system parameters *in situ*, say, by varying the control and Stark fields. While we used the well-studied rubidium isotopes, the proposed scheme allows for further generalization and improvement using other atomic isotopes, other atomic configurations, mixtures of more than two isotopes, monoatomic vapors with more than two control fields, etc. Adding more control parameters opens possibilities for

experimental implementation of nonlinear $\mathcal{PT}$-symmetric susceptibilities [27], as well as for creation of combined linear and nonlinear ones [28].

This work was supported by the Program of Introducing Talents of Discipline to Universities under Grant No. B12024, by NSF-China under Grants No. 11174080 and No. 11105052, as well as by the FCT Grants No. PEst-OE/FIS/UI0618/2011 and No. PTDC/FIS/112624/2009.

[1] N. N. Bogoliubov, J. Phys. (Moscow) **11**, 23 (1947); P. G. de Gennes, *Superconductivity of Metals and Alloys* (Benjamin, New York, 1965).
[2] T. Kato, *Perturbation Theory for Linear Operators* (Springer-Verlag, Berlin, 1980).
[3] C. M. Bender and S. Boettcher, Phys. Rev. Lett. **80**, 5243 (1998).
[4] C. M. Bender, S. Boettcher, and P. N. Meisinger, J. Math. Phys. (N.Y.) **40**, 2201 (1999); C. M. Bender, J. Brod, and M. E. Reuter, J. Phys. A **37**, 10139 (2004).
[5] A. Ruschhaupt, F. Delgado, and J. G. Muga, J. Phys. A **38**, L171 (2005).
[6] C. E. Rüter, K. G. Makris, R. El-Ganainy, D. N. Christodoulides, M. Segev, and D. Kip, Nat. Phys. **6**, 192 (2010).
[7] M. Kulishov, J. M. Laniel, N. Bélanger, J. Azaña, and D. V. Plant, Opt. Express **13**, 3068 (2005); Z. Lin, H. Ramezani, T. Eichelkraut, T. Kottos, H. Cao, and D. N. Christodoulides, Phys. Rev. Lett. **106**, 213901 (2011).
[8] L. Feng, M. Ayache, J. Huang, Y.-L. Xu, M.-H. Lu, Y.-F. Chen, Y. Fainman, and A. Scherer, Science **333**, 729 (2011).
[9] S. Longhi, Phys. Rev. A **82**, 031801 (2010).
[10] V. V. Konotop, V. S. Shchesnovich, and D. A. Zezyulin, Phys. Lett. A **376**, 2750 (2012).
[11] H. Benisty, A. Degiron, A. Lupu, A. De Lustrac, S. Chénais, S. Forget, M. Besbes, G. Barbillon, A. Bruyant, S. Blaize, and G. Lérondel, Opt. Express **19**, 18004 (2011).
[12] A. Regensburger, C. Bersch, M.-A. Miri, G. Onishchukov, D. N. Christodoulides, and U. Peschel, Nature (London) **488**, 167 (2012).
[13] A. Guo, G. J. Salamo, D. Duchesne, R. Morandotti, M. Volatier-Ravat, V. Aimez, G. A. Siviloglou, and D. N. Christodoulides, Phys. Rev. Lett. **103**, 093902 (2009).
[14] M. O. Scully, Phys. Rev. Lett. **67**, 1855 (1991); M. Fleischhauer, C. H. Keitel, M. O. Scully, C. Su, B. T. Ulrich, and S. Y. Zhu, Phys. Rev. A **46**, 1468 (1992).
[15] A. S. Zibrov, M. D. Lukin, L. Hollberg, D. E. Nikonov, M. O. Scully, H. G. Robinson, and V. L. Velichansky, Phys. Rev. Lett. **76**, 3935 (1996).
[16] D. D. Yavuz, Phys. Rev. Lett. **95**, 223601 (2005).
[17] N. A. Proite, B. E. Unks, J. T. Green, and D. D. Yavuz, Phys. Rev. Lett. **101**, 147401 (2008).
[18] C. O'Brien, P. M. Anisimov, Y. Rostovtsev, and O. Kocharovskaya, Phys. Rev. A **84**, 063835 (2011).
[19] Z. J. Simmons, N. A. Proite, J. Miles, D. E. Sikes, and D. D. Yavuz, Phys. Rev. A **85**, 053810 (2012).
[20] See, e.g., V. S. Letokhov, *Laser Conrol of Atoms and Molecules* (Oxford University Press, New York, 2007).
[21] Y. Bai, S. Slivken, S. R. Darvish, A. Haddadi, B. Gokden, and M. Razeghia, Appl. Phys. Lett. **95**, 221104 (2009).
[22] Y. Bai, S. R. Darvish, S. Slivken, W. Zhang, A. Evans, J. Nguyen, and M. Razeghi, Appl. Phys. Lett. **92**, 101105 (2008); M. Razeghi, IEEE J. Sel. Top. Quantum Electron. **15**, 941 (2009).
[23] J. Gea-Banacloche, Y. Q. Li, S. Z. Jin, and M. Xiao, Phys. Rev. A **51**, 576 (1995).
[24] D. Steck, ^{87}Rb and ^{85}Rb D Line Data, http://steck.us/alkalidata.
[25] See, e.g., C. M. Bender, G. V. Dunne, and P. N. Meisinger, Phys. Lett. A **252**, 272 (1999); J. K. Boyd, J. Math. Phys. (N.Y.) **42**, 15 (2001); J. M. Cerveró and A. Rodríguez, J. Phys. A **37**, 10167 (2004); K. G. Makris, R. El-Ganainy, D. N. Christodoulides, and Z. H. Musslimani, Phys. Rev. Lett. **100**, 103904 (2008); B. Midya, B. Roy, and R. Roychoudhury, Phys. Lett. A **374**, 2605 (2010).
[26] Here the complex propagation constant is related to the violation of Eq. (2) rather than to the $\mathcal{PT}$ symmetry breaking. With the accuracy 10^{-4}, the optimized susceptibility has the form $\chi_p = 0.2298 + 0.0076\cos\xi + i[0.0026 + 10^{-4}(4.0083\sin\xi + 1.8217\cos\xi)]$; i.e., its constant part results in the absorption of the light.
[27] F. Kh. Abdullaev, Y. V. Kartashov, V. V. Konotop, and D. A. Zezyulin, Phys. Rev. A **83**, 041805(R) (2011).
[28] Y. He, X. Zhu, D. Mihalache, J. Liu, and Z. Chen, Phys. Rev. A **85**, 013831 (2012).